

DSAL-GAN: DENOISING BASED SALIENCY PREDICTION WITH GENERATIVE ADVERSARIAL NETWORKS

Prerana Mukherjee^{†*} and Manoj Sharma^{‡*} Megh Makwana^{§*} Ajay Pratap Singh[‡],
 Avinash Upadhyay[‡] Akkshita Trivedi[‡] Brejesh Lall[§] Santanu Chaudhury[¶]
[†] IIT Sri City, [‡]CSIR-CEERI Pilani, [§]CCS Computers Pvt Ltd, [§]IIT Delhi, [¶]IIT Jodhpur .

[†] prerana.m@iiits.in, [‡] {mksnith, singhajay518, avinres, akkshitatrivedi}@gmail.com,

[§] meghmak95@gmail.com, [§] brejesh@ee.iitd.ac.in, [¶] schaudhury@gmail.com.

ABSTRACT

Synthesizing high quality saliency maps from noisy images is a challenging problem in computer vision and has many practical applications. Samples generated by existing techniques for saliency detection cannot handle the noise perturbations smoothly and fail to delineate the salient objects present in the given scene. In this paper, we present a novel end-to-end coupled Denoising based Saliency Prediction with Generative Adversarial Network (DSAL-GAN) framework to address the problem of salient object detection in noisy images. DSAL-GAN consists of two generative adversarial-networks (GAN) trained end-to-end to perform denoising and saliency prediction altogether in a holistic manner. The first GAN consists of a generator which denoises the noisy input image, and in the discriminator counterpart we check whether the output is a denoised image or ground truth original image. The second GAN predicts the saliency maps from raw pixels of the input denoised image using a data-driven metric based on saliency prediction method with adversarial loss. Cycle consistency loss is also incorporated to further improve salient region prediction. We demonstrate with comprehensive evaluation that the proposed framework outperforms several baseline saliency models on various performance benchmarks.

Index Terms— Denoising, Generative Adversarial Networks, Saliency, Joint optimization.

1. INTRODUCTION

Selective attentional processing involves suitable processing of visual stimuli to localize the salient objects in the image and hence it is an important area of research. The concept is highly inspired by the inherent working of the human visual system (HVS). In the visual cortex, every neuron responds to a particular section of the visual field. The receptive field (RF) is the area which is responsible for the perception of the visual stimuli. It responds to the center-surround difference

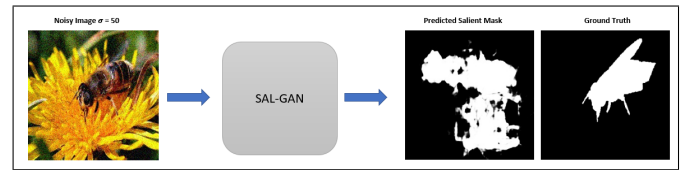


Fig. 1. Results of SAL-GAN (trained on clean data for saliency prediction) for noisy image as Input

detection corresponding to the object’s edges. As we progressively ascend to the higher levels in the visual cortex, the object representation is laid out in a hierarchical topography. This selective attentional processing or commonly termed as saliency prediction draws huge attention in the vision community due to its widespread applicability in various research domain areas such as adaptive image compression [1, 2], video summarization [3], image retargeting[4] etc. However, when the input image is distorted due to noise perturbations, the detection of the salient object becomes challenging as most of the saliency detection approaches [5] may fail to recognize the salient object in presence of noise and misclassify noise pixels as object pixels as shown in Fig. 1.

The closest work to ours is *SalGAN* which estimates the saliency map of an input image using a deep convolutional neural network (DCNN) utilizing a binary cross entropy (BCE) loss getting propagated across successive down-sampled saliency maps. Furtheron, the model is refined with the discriminator block which aligns the fake (generated saliency output) close to the real (ground truth saliency map) one. However, in presence of noise variations it is not able to handle the salient object prediction as shown in Fig. 1. To circumvent this problem, in this work we propose a novel end-to-end coupled Denoising based Saliency Prediction with Generative Adversarial Network (DSAL-GAN) framework. DSAL-GAN consists of coupled dual step generative adversarial network: i) In first generator step, we perform denoising of the input noisy image, and in the discriminator counterpart we check whether the output is a denoised image or ground truth original image, ii) In the second generator step, we predict saliency maps from raw pixels of an input denoised

*Equal Contribution

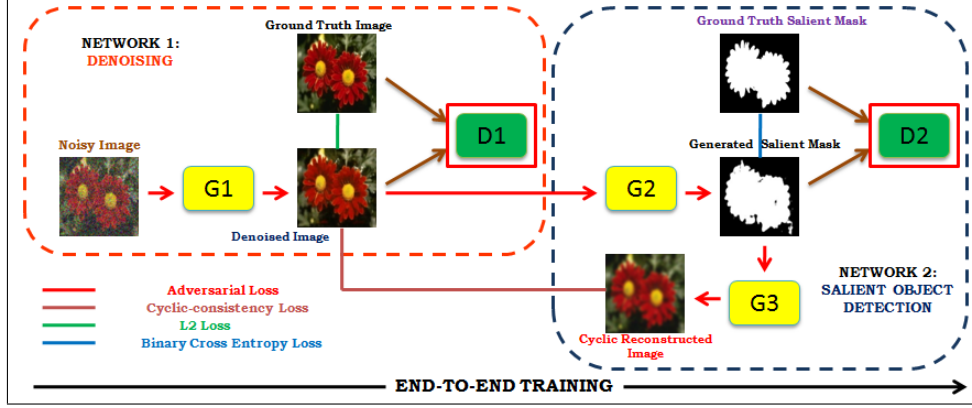


Fig. 2. End-to-End DSAL-GAN Network Architecture.

image, and in the discriminator counterpart we discriminate whether a saliency map is a predicted one or ground truth. Due to joint optimisation (end-to-end) training, DSAL-GAN generates the predicted saliency map which is indistinguishable with the ground truth and is capable of handling noisy images in a holistic manner.

In view of above discussions, the key contributions of this paper are:

1. Joint optimization of denoising and saliency prediction in a coupled end-to-end trainable GAN framework.
2. Use of cycle consistency loss to refine saliency prediction.
3. Exhaustive comparative analysis with several saliency baselines to demonstrate superior performance over various benchmark datasets.

Remaining sections in the paper are organized as follows. In Sec. 2, we outline the methodology we propose to provide a holistic framework for denoising and saliency prediction. In Sec. 3, we discuss experimental results and conclude the paper in Sec. 4.

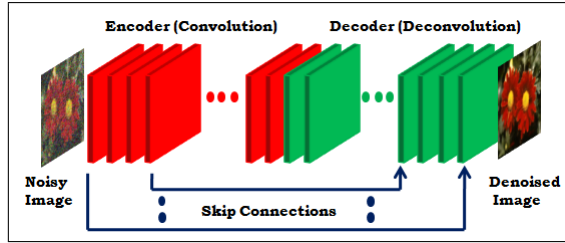


Fig. 3. RED-Net Generator Network Architecture [6].

2. METHODOLOGY

2.1. Problem Formation

The problem of denoising can mathematically be formulated as $x = D.y$. The x and y denote the noisy and clean image

(without noise perturbations) and D represents the noise matrix which degrades the clean image. Clean image y can be obtained by taking inverse of the noise matrix. The formulation to obtain denoised image y is:

$$y = D^{-1}.x = f_d(x) \quad (1)$$

Where f_d is denoising function. The saliency map can be obtained using the following equation:

$$z = f_{SOD}(f_d(x)) = f_{SOD}(y) \quad (2)$$

Where z is the saliency map of clean image y obtained using denoising function on x . The f_{SOD} function is responsible for localization of saliency map.

2.2. Image Denoising

As shown in the Fig. 2, the denoising network maps the noisy image x to a clean (denoised) image y . The generator $G1$ learns to generate image $y_{predicted}$ from input noisy image x , while the discriminator network $D1$ learns to differentiate between $y_{predicted} = y_p$ and y (Ground Truth). Here, the generator architecture is similar as given in [6], and shown in Fig. 3. The content loss (L2 Loss) of the generator can be represented as,

$$L_{Content}^{Denoising} = \frac{1}{n} \sum_{i=1}^N \| G1(x_i) - Y_i \|_2 \quad (3)$$

The adversarial loss can be formulated as,

$$L_{Adversarial}^{Denoising} = \frac{1}{n} \sum_{i=1}^N -\log D1(G1(x_i)) \quad (4)$$

Total loss for the denoising network is calculated as,

$$L^{Denoising} = L_{Content}^{Denoising} + w_1.L_{Adversarial}^{Denoising} \quad (5)$$

Table 1. Discriminator Network Architecture used for both Denoising and Salient Object Detection. s and p denote stride and padding respectively.

layers	Image
[layer 1]	conv1_a (1,1,3), s=1, p=1; ReLU conv1_b (3,3,32), s=1, p=1; ReLU pool1 (2,2), s=2, p=0
[layer 2]	conv2_a (3,3,64), s=1, p=1; ReLU conv2_b (3,3,64), s=1, p=1; ReLU pool2 (2,2), s=2, p=0
[layer 3]	conv3_a (3,3,64), s=1, p=1; ReLU conv3_b (3,3,64), s=1, p=1; ReLU pool3 (2,2), s=2, p=0
[layer 4]	fc4 (100); tanh
[layer 5]	fc5 (2); tanh
[layer 6]	fc6 (1); sigmoid

2.3. Saliency Object Detection

The network for saliency detection shown in the Fig. 2 is the extended version of the SalGAN [5]. The network is optimized for three different losses naming, content loss i.e., binary cross entropy (BCE), adversarial loss and cyclic consistency loss. Cyclic consistency loss is introduced to limit the space of possible mapping function. The three losses can be formulated as,

$$L_{BCE}^{SOD} = -\frac{1}{n} \sum_{i=1}^N (z_i \cdot \text{Log}(z_i^p) + (1 - z_i) \cdot \text{Log}(1 - z_i^p)) \quad (6)$$

$$L_{Adversarial}^{SOD} = \frac{1}{n} \sum_{i=1}^N -\text{Log} D2(G2(G1(x_i))) \quad (7)$$

$$L_{Cyclic}^{SOD} = \frac{1}{n} \sum_{i=1}^N \| G3(G2(G1(x_i))) - G1(x_i) \|_2 \quad (8)$$

The overall joint optimization objective of training the network can be formulated as,

$$L^{SOD} = L_{BCE}^{SOD} + w_2 \cdot L_{Adversarial}^{SOD} + w_3 \cdot L_{Cyclic}^{SOD} \quad (9)$$

The specification of discriminator [6] architecture used for denoising and salient object detection is given in Table. 1 respectively. The generator [6] architecture used for salient object detection is given in Table. 2. The architecture given in Fig. 3 is also used for generator3 (G3) to learn reverse mapping from saliency map to corresponding clean image.

2.4. Joint Optimisation of Denoising and Saliency Prediction

We initialise end-to-end coupled network i.e., DSAL-GAN for joint optimization of denoising and saliency prediction by

Table 2. Generator Network Architecture used for Salient Object Detection. s and p denote stride and padding respectively.

layers	Image
[layer 1]	conv1_a (1,1,64), s=1, p=1; ReLU conv1_b (3,3,64), s=1, p=1; ReLU pool1 (2,2), s=2, p=0
[layer 2]	conv2_a (3,3,128), s=1, p=1; ReLU conv2_b (3,3,128), s=1, p=1; ReLU pool2 (2,2), s=2, p=0
[layer 3]	conv3_a (3,3,256), s=1, p=1; ReLU conv3_b (3,3,256), s=1, p=1; ReLU conv3_c (3,3,256), s=1, p=1; ReLU pool3 (2,2), s=2, p=0
[layer 4]	conv4_a (3,3,512), s=1, p=1; ReLU conv4_b (3,3,512), s=1, p=1; ReLU conv4_c (3,3,512), s=1, p=1; ReLU pool4 (2,2), s=2, p=0
[layer 5]	conv5_a (3,3,512), s=1, p=1; ReLU conv5_b (3,3,512), s=1, p=1; ReLU conv5_c (3,3,512), s=1, p=1; ReLU
[layer 6]	conv6_a (3,3,512), s=1, p=1; ReLU conv6_b (3,3,512), s=1, p=1; ReLU conv6_c (3,3,512), s=1, p=1; ReLU upsample6 (2,2), s=2, p=0
[layer 7]	conv7_a (3,3,512), s=1, p=1; ReLU conv7_b (3,3,512), s=1, p=1; ReLU conv7_c (3,3,512), s=1, p=1; ReLU upsample7 (2,2), s=2, p=0
[layer 8]	conv8_a (3,3,256), s=1, p=1; ReLU conv8_b (3,3,256), s=1, p=1; ReLU conv8_c (3,3,256), s=1, p=1; ReLU upsample8 (2,2), s=2, p=0
[layer 9]	conv9_a (3,3,128), s=1, p=1; ReLU conv9_b (3,3,128), s=1, p=1; ReLU upsample9 (2,2), s=2, p=0
[layer 10]	conv10_a (3,3,64), s=1, p=1; ReLU conv10_b (3,3,64), s=1, p=1; ReLU output (1,1,1), s=1, p=0; Sigmoid

taking pre-trained weights of network1 and network2 as given in Fig. 2. We consider pre-trained weights as initial weights to finetune the combined network into an end-to-end manner.

3. EXPERIMENTS AND RESULTS

3.1. Datasets

We have trained our model on benchmark datasets such as SOD [7], MSRA 10k [8] and ECSSD [9]. We have created a synthetic dataset using the input images from these datasets and degraded them using Gaussian noise with variance ranging from [10, 30, 50, 80]. The experimental results are obtained on these synthesized datasets for various baseline saliency detection models.

3.2. Results and Discussion

The comparison of DSAL-GAN with other state-of-the-art saliency detection framework is shown in Fig. 4 (*for illustration purposes we have shown results for $\sigma=50$ only*). The performance of the proposed framework shows performance gain over the other state of the art saliency detection frameworks for noisy images. Table 3 represents the comparative analysis between these techniques over several performance evaluation metrics average F-measure (aveF), maximum F-measure (maxF), Area under the curve (AUC), Mean Average

Error (MAE). The performance of the proposed framework shows far more effective detection of salient regions as compared to the state of the art saliency detection frameworks for noisy images. The proposed framework provides an improvement of $\sim 10\%$ and 16% in aveF, $\sim 9.5\%$ and 16% in maxF, and $\sim 9.6\%$ and 21% in AUC and a drop of $\sim 38\%$ and 47% in MAE with respect to Sal-GAN and Deep Saliency respectively for images having noise variance, $\sigma = 50$. Performance gain in AUC represents the increase in the pixel classification accuracy. It can be evidently observed that the proposed framework outperforms various state of the art saliency detection frameworks on noise induced synthetic dataset. The experimental results validates that there is decrease in AUC with increase in noise as shown in Tab. 4.

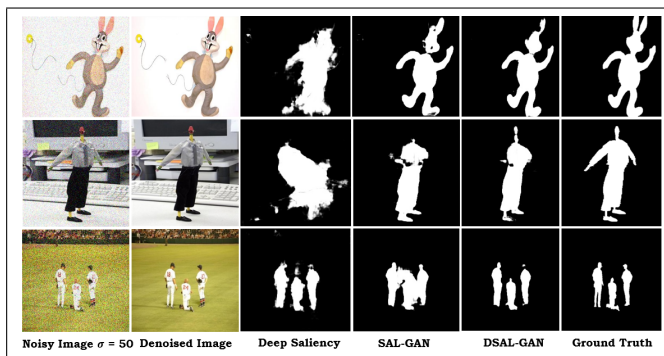


Fig. 4. From left to right, a) Noisy input image, b) Denoised image, c) Deep saliency [10], d) Sal-GAN [6], e) Proposed DSAL-GAN, f) Ground Truth.

Baseline: We have benchmarked the performance of DSAL-GAN against the state-of-the-art frameworks like Sal-GAN and Deep Saliency on our synthetic dataset. We observe a performance drop in F1-score, AUC, MAE metrics for Sal-GAN and Deep Saliency, when they are trained on our synthetic dataset.

4. CONCLUSION

We have performed saliency detection on the noisy images using two generative-adversarial networks trained end-to-end. The denoising network utilized skip connection based convolutional network as a generative framework whereas the saliency detection network used a simple encode-decoder based convolutional network as a generative framework. The saliency detection network was optimized with a combination of three losses namely: content loss, adversarial loss and cycle consistency loss. The denoising network was optimized on content loss and adversarial loss. The proposed network performed reasonably well in comparison to other state-of-the-art saliency detection methods. We have also demonstrated that the use of cycle-consistency loss while training the saliency detection network has enhanced the results to a great extent.

Table 3. Comparison of algorithms on different benchmark datasets for $\sigma=50$.

Algorithms		MSRA-10K	ECSSD	SOD
DSAL-GAN	aveF \uparrow	0.6523	0.6328	0.6019
	maxF \uparrow	0.7343	0.7235	0.7104
	AUC \uparrow	0.9012	0.8503	0.8309
	MAE \downarrow	0.0923	0.1382	0.1611
SalGAN	aveF \uparrow	0.6008	0.5608	0.5493
	maxF \uparrow	0.7123	0.6431	0.6218
	AUC \uparrow	0.8221	0.7818	0.7523
	MAE \downarrow	0.1699	0.2308	0.2407
Deep Saliency	aveF \uparrow	0.5818	0.5100	0.5004
	maxF \uparrow	0.7010	0.5923	0.5757
	AUC \uparrow	0.6523	0.7404	0.7308
	MAE \downarrow	0.2023	0.2646	0.2728

Table 4. AUC for different standard deviation (σ) values on benchmark datasets.

Standard Deviation	$\sigma=10$	$\sigma=30$	$\sigma=50$	$\sigma=80$
MSRA-10k	0.939	0.921	0.901	0.4512
ECSSD	0.9006	0.8714	0.8503	0.4163
SOD	0.8814	0.8627	0.8309	0.3942

5. REFERENCES

- [1] Ji Hwan Park, Ievgeniia Gutenko, and Arie E Kaufman, “Transfer function-guided saliency-aware compression for transmitting volumetric data,” *IEEE Transactions on Multimedia*, 2017.
- [2] Shengxi Li, Mai Xu, Yun Ren, and Zulin Wang, “Closed-form optimization on saliency-guided image compression for hevc-msp,” *IEEE Transactions on Multimedia*, vol. 20, no. 1, pp. 155–170, 2018.
- [3] Ioannis Mademlis, Anastasios Tefas, and Ioannis Pitas, “Regularized svd-based video frame saliency for unsupervised activity video summarization,” in *2018 IEEE International Conference on Acoustics, Speech and Signal Processing (ICASSP)*. IEEE, 2018, pp. 2691–2695.
- [4] Yinzuo Zhou, Luming Zhang, Chao Zhang, Ping Li, and Xuelong Li, “Perceptually aware image retargeting for mobile devices,” *IEEE Transactions on Image Processing*, vol. 27, no. 5, pp. 2301–2313, 2018.
- [5] Junting Pan, Cristian Canton Ferrer, Kevin McGuinness, Noel E O’Connor, Jordi Torres, Elisa Sayrol, and Xavier Giro-i Nieto, “Salgan: Visual saliency prediction with generative adversarial networks,” *arXiv preprint arXiv:1701.01081*, 2017.

- [6] Xiao-Jiao Mao, Chunhua Shen, and Yu-Bin Yang, “Image restoration using convolutional auto-encoders with symmetric skip connections,” *CoRR*, vol. abs/1606.08921, 2016.
- [7] Vida Movahedi and James H Elder, “Design and perceptual validation of performance measures for salient object segmentation,” in *Computer Vision and Pattern Recognition Workshops (CVPRW), 2010 IEEE Computer Society Conference on*. IEEE, 2010, pp. 49–56.
- [8] Ming-Ming Cheng, Niloy J. Mitra, Xiaolei Huang, Philip H. S. Torr, and Shi-Min Hu, “Global contrast based salient region detection,” *IEEE TPAMI*, vol. 37, no. 3, pp. 569–582, 2015.
- [9] Qiong Yan, Li Xu, Jianping Shi, and Jiaya Jia, “Hierarchical saliency detection,” in *Proceedings of the IEEE Conference on Computer Vision and Pattern Recognition*, 2013, pp. 1155–1162.
- [10] Xi Li, Liming Zhao, Lina Wei, Ming-Hsuan Yang, Fei Wu, Yueting Zhuang, Haibin Ling, and Jingdong Wang, “Deepsaliency: Multi-task deep neural network model for salient object detection,” *CoRR*, vol. abs/1510.05484, 2015.